Desalination and Water Treatment
www.deswater.com
doi: 10.5004/dwt.2020.25832

193 (2020) 235–250
July

Comparison of membrane fouling and cleaning in one-pass reverse osmosis and two-pass nanofiltration approaches to seawater desalination

Dian Tanuwidjaja[a], Xue Jin[a], Xiaofei Huang[a], Catalina Marambio-Jones[a], Anna Jawor[a], Minglu Zhang[b], Sunny Jiang[b], Robert Cheng[c], Eric M.V. Hoek[a,*]

[a]*Department of Civil and Environmental Engineering, Institute of the Environment and Sustainability and California NanoSystems Institute, University of California, Los Angeles, California 90095, USA, Tel. +1-310-794-7124; Fax: +1-310-206-2222; email: emvhoek@ucla.edu (E.M.V. Hoek), Tel. +1-562-570-2357; email: dian.tanuwidjaja@lbwater.org (D. Tanuwidjaja), Tel. +1-541-737-7968; email: xue.jin@oregonstate.edu (X. Jin), Tel. +1-760-901-2500; email: XHuang@hydranautics.com (X. Huang), Tel.+1-626-377-8804; email: drmarambio@coronacharter.org (C. Marambio-Jones), Tel. +1-951-892-8563; email: anna.jawor@polyceramembranes.com (Anna Jawor)*
[b]*Department of Civil and Environmental Engineering, University of California, Irvine, California 92697, USA, email: 88652745@qq.com (Minglu Zhang), Tel. +1-949-824-5527; email: sjiang@uci.edu (S. Jiang)*
[c]*Long Beach Water Department, Long Beach, California 90806, USA, Tel. +1-760-398-2651; email: RCheng@cvwd.org (R. Cheng)*

Received 19 August 2019; Accepted 12 March 2020

ABSTRACT

A recent innovation in seawater desalination is the use of multi-stage and multi-pass combinations of nanofiltration (NF) and reverse osmosis (RO) membranes. One example of this approach is the "Long Beach method," in which seawater passes through two different types of NF membranes to produce potable water. After several years of pilot studies comparing the performance of two-pass NF and single-pass RO systems, a number of membrane elements were sacrificed for autopsy analyses. The selected membranes represent different stages of operation including (1) new, (2) fouled, and (3) cleaned membranes. Used NF and RO spiral wound elements were removed from the first and last positions of the demonstration plant. Although operating data suggested no outward signs of membrane fouling – inorganic, organic, and bacterial accumulation were identified on all membranes. First pass RO and NF membranes contained similar amounts of deposited solids, while significantly fewer solids were found on second pass NF membranes. Viable, culturable marine bacteria were observed on all fouled and cleaned membranes, indicating that bacterial colonization of seawater NF/RO membranes was not (a) detected by plant performance monitoring devices, (b) prevented by microfiltration and chlorination, or (c) removed by chemical cleaning. Chemical cleaning recovered the measurable performance of both first pass RO and second pass NF membranes, but was relatively ineffective at removing deposited solids from first-pass NF membranes. Therefore, chemical-cleaning methods may need to be tailored and optimized more specifically for NF membranes used in seawater desalination.

Keywords: Reverse osmosis; Nanofiltration; Seawater; Desalination; Fouling; Cleaning

* Corresponding author.

1944-3994/1944-3986 © 2020 Desalination Publications. All rights reserved.

1. Introduction

Less than 0.5 percent of all the freshwater on Earth is accessible surface and groundwater, yet nearly all of the water used by humans is derived from this limited supply [1]. Serious consideration is now given to seawater desalination as a viable source of potable water; however, the application of seawater desalination is limited by the high cost of desalinated water (relative to conventionally treated, local freshwater sources) and environmental concerns such as (1) impingement and entrainment of marine organisms at feed water intakes, (2) marine ecosystem impacts from brine discharge, and (3) high energy demand and associated carbon footprint.

The first two issues can be minimized with appropriately engineered subsurface intakes and brine discharge systems or by co-location with power plant cooling water intake and outfall systems, but the high cost, energy demand, carbon footprint remain concerns. Operating costs, energy demand, and carbon footprint of seawater RO plants are driven by the high pressure needed to drive water through the RO membranes, which is almost entirely due to the osmotic and hydraulic pressure drops across the membrane [2]; the former is intrinsic to the feedwater dissolved solids concentration, permeate flux, and product water recovery while the latter is a function of the membrane permeability and permeate flux. Several recent advancements in seawater reverse osmosis (SWRO) membrane module and process technologies have reduced energy demands without sacrificing separation performance, including high-flux, high-rejection SWRO membranes, and high-efficiency energy recovery devices [3,4]. These along with coupling SWRO plants to renewable energy sources can reduce carbon footprint. Another approach involves the use of multi-pass membrane systems employing less selective, but more hydraulically efficient desalting membranes [5]. The multi-pass approach offers other potential advantages, including the use of lower-pressure pumps, fittings, valves, and vessels, which are cheaper than high-pressure analogs used in "single-pass" SWRO plants. We use quotations around "single-pass" because many state-of-the-art seawater RO plants already use multi-pass configurations to achieve acceptable boron removal.

The Long Beach Water Department (LBWD) operated a prototype 1 mega-L/d (300,000 gallon/d), two-pass seawater nanofiltration (SWNF) desalination plant from 2006 to 2009. Initial pilot studies were conducted to prove the operational feasibility of the LBWD's two-pass SWNF process to produce acceptable quality desalinated water [5]. The prototype study evaluated the plant level performance of a two-pass SWNF process side-by-side with a conventional "single-pass" SWRO system. Later studies evaluated parallel SWNF systems operating with different pretreatment combinations such as microfiltration alone and in combination with ultraviolet irradiation or continuous dosing of chlorine dioxide.

Much is known about the fouling behavior of traditional "single-pass" SWRO plants. For example, it is known that plant level specific flux is not a rigorous or reliable indicator of membrane fouling because highly permeable modern RO membranes do not exhibit system wide flux decline even when it is ongoing for many months [6]. As fouling progresses, more water permeates elements further down the system and the high permeability allows the system average flux to appear constant [7]. Also, it is widely accepted that bacteria colonize NF/RO membranes without causing outward symptoms of membrane fouling. If viable, but not culturable bacteria adhere to NF/RO membrane surfaces there may be no symptoms of fouling until environmental conditions change adequately to stimulate the resuscitation process [8,9]. Alternatively, if viable, culturable (i.e., metabolically active) bacteria colonize the membranes, biofilm formation might be rapid, and catastrophic following a sudden influx of nutrients from a coastal algae bloom. The key question motivating this study was, "Are there any fundamental differences between the fouling behavior of conventional SWRO membranes and LBWD's patented two-pass SWNF process (a.k.a., LBWD NF^2)" [10]; we hypothesized that no major differences would emerge.

Herein, we present the results from physical, chemical, and biological analyses performed on seawater NF and RO membranes obtained after the LBWD's prototype study. Three different types of membranes obtained from two different locations within the treatment trains were investigated, a lead and tail element from the (1) single-pass SWRO system, (2) the first pass of the two-pass SWNF system, and (3) the second-pass of the two-pass SWNF system. The rest of the membrane modules were subject to commercial chemical cleaning. Upon return from cleaning, a lead element from each configuration was sacrificed for autopsy analyses to assess the effectiveness of chemical cleaning.

2. Materials and methods

2.1. One-pass SWRO and two-pass SWNF systems

Seawater for the prototype facility is pumped from the Los Angeles Department of Water and Power (LADWP) Haynes Generating Station cooling water channel. The cooling water channel seawater intake is located within the Long Beach Marina, which is situated just west of the mouth of the San Gabriel River. The source water quality is characteristic of coastal seawater off the coast of Southern California. Table 1 presents the Long Beach raw water quality at the intake and a previously published seawater quality analysis [11].

The source water undergoes several pretreatment processes before reaching the NF/RO desalination stage. These occur in the following sequence: (1) trash racks at the channel intake screen out coarse materials, (2) 300 μm self-backwashing strainers, (3) chlorination by sodium hypochlorite, and (4) 0.1 μm microfiltration (MF) system (Pall Microza, East Hills, NY). Water exiting the MF filtrate break-tank is de-chlorinated with sodium metabisulfite to achieve a chlorine residual of <0.1 mg/L and then passes through 1 μm cartridge filters. The SWNF membrane used in the first pass was designated as "NFP1" (NF90, Dow Water Solutions, Midland, MI) and in the second pass was designated as "NFP2" (NE90, CSM, Korea), while the seawater RO membrane (SWC3+, Hydranautics, Oceanside, CA) was designated as SWRO. All membranes were described by the respective manufacturers to be "polyamide composite" membranes.

Table 1
Water quality for raw water intake and "typical seawater" [7]

Primary regulated ions	Units	LBWD raw		Typical seawater
		Average	Standard deviation	
Arsenic	mg/L	ND	ND	0.003
Barium	mg/L	ND	ND	0.03
Cadmium	mg/L	ND	ND	0.00011
Chromium, total	mg/L	ND	ND	0.00005
Chromium, VI	mg/L	NA	NA	NA
Copper	mg/L	ND	ND	0.003
Fluoride	mg/L	0.68	0.00	1.3
Lead	mg/L	ND	ND	0.00003
Mercury	mg/L	ND	ND	0.00003
Nitrate	mg/L	ND	ND	NA
Selenium	μg/L	ND	ND	0.004
Other ions				
Aluminum	mg/L	0.053	0.012	0.01
Ammonia	mg/L	0.1	0.0	0.0097
Bicarbonate	mg/L	113	0	NA
Boron	mg/L	3.9	0.0	4.6
Bromide	mg/L	59.8	0.8	65
Calcium	mg/L	411	3	400
Carbonate	mg/L	ND	ND	NA
Chloride	mg/L	18,426	136	19,000
Hardness, total	mg/L	6,189	40	NA
Hydrogen sulfide	mg/L	ND	ND	NA
Iron, total	mg/L	0.1	0	0.01
Iron, dissolved	mg/L	ND	ND	NA
Magnesium	mg/L	1,254	7	1,350
Manganese	mg/L	ND	ND	0.002
Nickel	mg/L	ND	ND	0.002
Phosphate	mg/L	0.14	0.02	0.07
Potassium	mg/L	372	2	380
Silica (SiO_2) total	mg/L	NA	NA	NA
Silica (reactive)	mg/L	0.81	0.07	NA
Silica (dissolved)	mg/L	0.41	0.01	NA
Silver	pg/L	ND	ND	0.00004
Sodium	mg/L	10,015	55	10,500
Strontium	mg/L	NA	NA	8
Sulfate	mg/L	2,335	13	2,654.3
Sulfide	mg/L	ND	ND	NA
Vanadium	mg/L	ND	ND	0.002
Zinc	mg/L	ND	ND	0.01

A single pretreated water source with total dissolved solids (TDS) concentration of about 34 g/L was supplied to both trains shown in Fig. 1. The single-pass SWRO process was arranged in two stages. The concentrate from stage 1 fed into stage 2 to achieve higher recovery, with a combined permeate TDS limit of ~0.35 g/L. The maximum allowable operating pressure of the SWRO membrane was 83 bar (1,200 psi), while the NF membranes were limited to 41 bars (600 psi) per manufacturer specifications. Both single-pass SWRO and two-pass SWNF trains were operated at a series of different operating conditions; hence, the operating pressure, permeate flux, and recovery of NFP1, NFP2, and SWRO were not held constant over the operational period.

The NF^2 process was arranged in two passes; each pass had two stages. First, dechlorinated MF filtrate was blended with brine from the second pass system and pressurized to ~33 bar (~480 psi) by primary pumps. This diluted seawater feed with TDS of about 30 g/L passed through NFP1 membranes. Pass 1-stage 1 performed the preliminary desalination of the seawater. Pass 1-stage 2 recovered additional water from the pressurized concentrate to increase the recovery of pass 1 permeate. The flow dynamics were unchanged from first to second stages because the same number of parallel pressure vessels was maintained in both stages. A high-efficiency energy recover device (Energy Recovery Inc., San Leandro, CA) transferred up to 97% of pass 1 – stage 2 brine pressure back to the feed flow. Combined permeate from both stages of pass 1 served as the feed for pass 2. Second, NFP1 permeate was repressurized to ~15 bar (~217 psi) and passed through NFP2 membranes. The goal for pass 1 and 2 combined permeate TDS goal <0.35 g/L based on the TDS of potable water currently delivered to LBWD's customers. Under this treatment scheme, NFP1 permeate TDS was ~3–4 g/L, and blended NFP1 and NFP2 permeate ranged from ~0.2 to 0.3 g/L – both depending on system operating conditions. The maximum operating pressure of the NF^2 process is 41 bar (600 psi), which limited the total product water recovery.

2.2. Membrane removal and autopsy preparation

After 2 y of operation, the membranes from the prototype were removed from the vessels and sent out to a commercial cleaning service. Additionally, two batches of membranes were sent to the University of California, Los Angeles (UCLA) Nanomaterials and Membrane Technology Research (NanoMeTeR) Laboratory for autopsy. The first batch of membrane elements consisted of six used membrane elements that were removed from the plant immediately after operation ceased. Each of the six elements represents the following:

- the first element in series from NF pass 1, stage 1,
- the last element in series from NF pass 1, stage 2,
- the first element in series from NF pass 2, stage 1,
- the last element in series from NF pass 2, stage 2,
- the first element in series from SWRO stage 1, and
- the last element in series from SWRO stage 2.

The second batch of membrane elements consisted of two membrane modules after cleaning by Siemens. These two membranes included the first element from NF pass 1 stage 1 and the first element from SWRO stage 1.

Upon receipt at UCLA, all elements were placed in the vertical position and drained for about 30 min. The element inlet and outlet were noted and marked to record the feed/brine flow direction. The two caps at the ends of the elements were cut with a circular saw and removed with hammer and

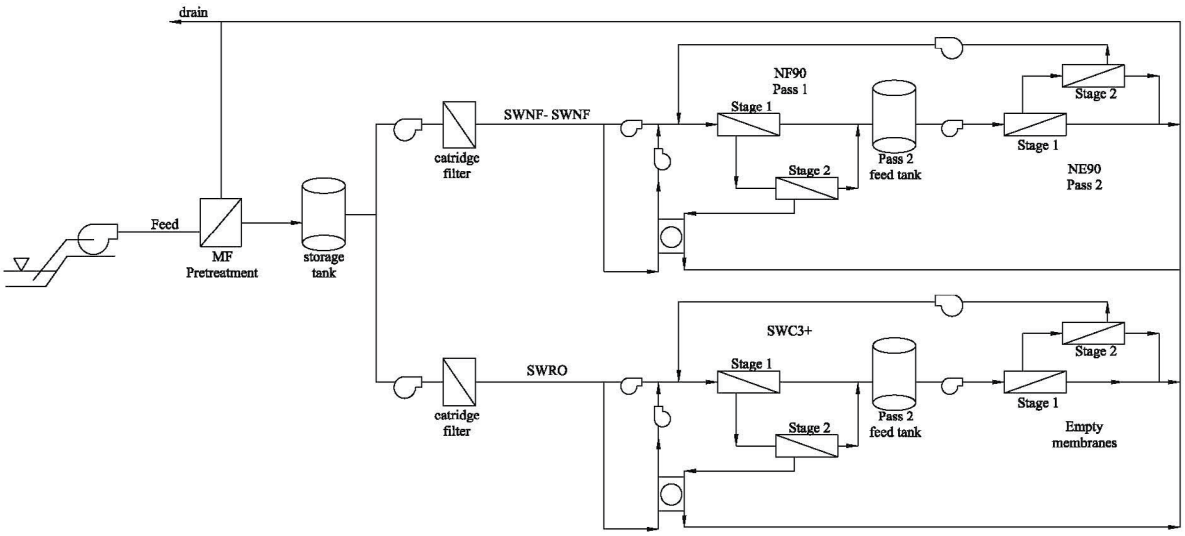

Fig. 1. Schematic of Long Beach Water Department prototype seawater desalination facility.

chisel. Then, the shell was also cut using a circular saw, and removed using a hammer and chisel. The fiberglass shell of each element was removed, and the exterior of the elements was examined carefully.

2.3. Physical inspection and analyses

After removing the fiberglass shell, elements were unrolled, and photographs were taken with a handheld digital camera (Canon SD700 IS, Canon, USA) to record various steps of the autopsy processes. The number of leaves was counted in each element. Leaf lengths, leaf widths, and glue line widths were recorded with a tape measure. Spacer filament thickness, separation, and orientation were measured using a micro-caliper. Spacer porosity was determined as follows. The solid volume of spacers was obtained by measuring the total volume of water displaced by submerging a small sample of spacer into a 25 mL graduated cylinder partially filled with laboratory deionized water. The porosity of the spacer was calculated from the ratio of solid volume to total volume (=sample length × width × thickness).

Measurements of total and combustible solids were carried out based on Standard Method 2540D [12]. In this procedure, 45 square inches of membrane surface area was scraped using a sterile blade. The solids removed from the surface of the membrane by the blade were rinsed into ceramic dishes. The samples were then dried in the oven for 24 h at 105°C, cooled, and weighed. Ceramic dishes were then placed in a furnace at 550°C for 1 h, cooled, and reweighed. The dry weight (after oven drying) gave the total solids. Total solids minus the mass of solids remaining after the furnace (non-volatile solids) gave the volatile solids.

2.4. Microscopic and spectroscopic analyses

Digested samples of extracted solids were analyzed by inductively coupled plasma optimal emission spectrometry, ICP-OES, (Model TJA Radial IRIS 1000 ICP OES, Perkin Elmer; Waltham, MA, USA) following acid digestion using HNO_3/HCl (Standard Method 3030F-Recoverable) [12]. In preparing ICP analysis, the solids were scraped from the surface of the membrane and rinsed into a 100 mL beaker. Inside the beaker, 2 mL of 50% HNO_3 and 10 mL of 50% HCl were added to the suspension. The suspension was heated on a hot plate until sample was reduced to ~40 mL, making certain the water did not boil. The sample was cooled, filtered (0.45 μm membrane), and transferred to a volumetric flask where the volume was adjusted to 50 mL with deionized water. The "Multielement Standard US EPA (23 elements)" (GFS Chemicals, Powell, OH, USA) with multiple dilution (1, 5, 10, and 20 mg/L) was used to provide standards for the ICP analysis.

Membrane samples were also cut out and dried overnight inside a desiccator. Spectra of these dried fouled NF/RO membranes were obtained by a Fourier transform infrared spectrometer (JASCO, FT/IR-670 Plus, Tokyo, Japan), equipped with a Seagull™ (JASCO Corporation, Tokyo, Japan) variable angle reflection accessory with Germanium attenuated total reflectance (ATR) crystal kit installed. The incident angle was set at 42°. Single-beam spectra took 100 scans at 4 cm^{-1} resolution for each sample. The obtained original spectra were baseline corrected, and CO_2 characteristic peak from the air was eliminated using Spectra Manager software (Version 1.53.04, JASCO Corporation, Tokyo, Japan).

Unused, fouled, and cleaned membranes were also analyzed by scanning electron microscopy, SEM (Hitachi S-4700, Pleasanton, CA). Before the SEM analysis, dried samples were sputter-coated with a mixture of gold and palladium. Magnifications used were varied from 100 to 10,000×. While SEM images were obtained, energy dispersive X-ray (EDX) spectroscopy (equipped with the SEM) was used to determine the elemental compositions of each membrane sample.

2.5. Biological analyses

Live and dead staining analyses were also performed. Samples were cut from inlet and outlet locations of opened elements. Small pieces of membrane sample were stained

using SYTO® 9 green-fluorescent nucleic acid stain and propidium iodide red-fluorescent nucleic acid stain (Live/Dead BacLight Bacterial Viability Kit, Invitrogen, Oregon) for 10 min. The SYTO 9 and propidium iodide stain were mixed in the same amount, such that all bacteria with intact cell walls stained fluorescent green, and bacteria with damaged cell walls stained fluorescent red. After 10 min, samples were removed from stain solutions, and attached onto a glass slide. The prepared stained sample slides were mounted onto a fluorescent microscope (Olympus, BX51WI, Olympus Corporation, Center Valley, PA) and imaged using both green and red filter channels. Images were captured by CCD camera installed on the top of the microscope. Bacterial colonization was evaluated by visually counting the number of cells attached to the membranes surfaces.

Microorganisms on the surface of open element membrane sheets were transferred using sterile inoculating loops. A streak was made over a sterile Difco marine agar (BD, Sparks MD, USA) plate to spread out organisms. The streaked plates were placed into an incubator for 72 h at 37°C. Subsequently, individual bacterial colonies were isolated on artificial seawater plates with 2.5 g/L of peptone and 0.5 g/L of yeast extract.

For phylogenetic analysis, a single colony from each bacterium was inoculated into 0.5 ml of sterile DI water. The colony was suspended by pipeting and boiled for 10 min to release DNA from the cells. The boiling lysate was diluted 1:10 and 1:100 times using sterilized DI water. One microliter of each dilution was used for polymerase chain reaction (PCR) using universal 16S rRNA gene primers [13]. Primers 27F (5′-AGA GTT TGA TCM TGG CTC AG-3′) and 1492R (5′-GGT TAC CTT GTT ACG ACT T-3′) amplify a 1,500-bp region of the 16S rRNA gene. The PCR mixture contained 1 × PCR buffer (Lucigen, Middleton, WI), 2.5 mM $MgCl_2$, 4 × 200 μM deoxynucleoside triphosphates, 400 nM each forward and reverse primer, and 1 U of EconoTaq (Lucigen) in a total of 25 mL reaction. The PCR was performed using GeneAmp 2700 PCR system (Applied Biosystems, CA) with the following thermal profile: initial denaturation at 94°C for 2 min followed by 30 cycles of 94°C for 1 min, 55°C for 1 min, and 72°C for 1.5 min, with a final extension at 72°C for 10 min and a hold at 4°C. The PCR amplicons were viewed by gel electrophoresis. The bands were extracted from the gel and purified using Zymoclean Gel DNA Recovery Kit (Zymo Research, CA). The purified PCR amplicons were used for direct sequencing using 27F, 533F, and 1492R primer, respectively, and BigDye 3.1 sequencing kit following manufacturers' protocols (Applied Biosystems, Foster City, CA). The final reactions were submitted to Laragen, Inc., (Los Angeles, CA) for sequencing run using ABI prism 3100 capillary sequencing.

Sequences were initially compared to the available databases by using the BLAST (basic local alignment search tool) network service (GenBank) to determine their approximate phylogenetic affiliations and orientation. Partial sequences were then compiled and aligned with 16S rRNA sequences. The phylogenic tree was constructed in TreeView. The GenBank accession numbers for the sequences are as follows, FJ652063, FJ654735, FJ654736, and FJ654737.

2.6. Membrane cleaning

Membrane samples cut out from the fouled membranes received by UCLA were mounted into a laboratory scale flat sheet tester (described in section 2.7. Separation performance testing) and sequentially rinsed with deionized water, a NaOH solution (pH ~12) and a citric acid solution (2%, pH ~4) at 25°C. Sufficient pressure was applied to recirculate water through the laboratory desalination simulator modules without permeation. After cleaning, the membranes were rinsed again with deionized water, followed by immediate performance testing as described below.

The membrane elements after being commercially cleaned (Siemens Water Technologies, Warrendale, PA) were also received by UCLA and analyzed. The Siemens cleaning procedure included the following steps.

- Deionized (DI) water was recirculated through the elements to eliminate large particulate matter stuck on the membranes or trapped by the spacers.
- Hot water (43°C–49°C) with a high pH (10.5–11) (Avista P111, Avista Technologies, San Marcos, CA) was circulated at through the elements for 2 h.
- Hot soft water (43°C–49°C) with a low pH (2.5–3.5) (Avista L403, Avista Technologies, San Marcos, CA) at was circulated through the elements for 2 h.

The membranes, received as sealed spiral wound elements, were autopsied and analyzed as described in the section 2.2 (Membrane removal and autopsy preparation). Small membrane samples were cut and mounted in the flat sheet tester for subsequent performance testing.

2.7. Separation performance testing

Membrane separation performance testing employed a custom fabricated bench-scale crossflow RO flat sheet tester previously described by Jin et al [14]. Six plate-and-frame membrane modules were designed with individual membrane area of 19 cm^2 (7.6 cm long by 2.5 cm wide) each, and a channel height of 2 mm. Water was maintained well mixed in the feed tank by magnetic stirring. The feed water was pressurized by a diaphragm pump (Hydracell, Wanner Engineering, Minneapolis, MN) outfitted with a custom flow dampener to maintain steady feed flow. The feed water temperature was maintained at 25°C ± 0.1°C by a laboratory recirculating heater/chiller (NTE RTE7, Fisher Scientific, Pittsburgh, PA). Backpressure regulators and bypass valves controlled feed water hydraulic pressure and crossflow velocity for each side individually. Permeate flow rate was monitored by a digital flowmeter (Optiflow 1000, Agilent Technology, Foster City, CA).

At the start of each experiment, the pure water permeability was determined by measuring the water flux over a range of applied pressures (400–800 psi). Flux was determined from the measured flow rate divided by the membrane area. Water permeability (A) was calculated from the flux (J) divided by the applied pressure (ΔP). Next, the membranes were equilibrated with 32 g/L NaCl solution for at least 1 h until steady flux was achieved. Observed salt rejection ($R = 1 - \kappa_p/\kappa_f$) was determined from feed (κ_f)

and permeate (κ_p) conductivities measured using a conductivity electrode (Accumet 13-620-160, Fisher Scientific, Pittsburgh, PA) attached to a pH/conductivity meter (Accumet, Fisher Scientific, Pittsburgh, PA). Salt permeability (B) was calculated from the observed rejection and flux via $B = J(1 - R)/R$.

3. Results and discussion

3.1. Historical operating data

The prototype two-pass NF plant and single-pass RO plants were tested across a range of operating conditions to evaluate impacts on energy demand and product water quality. The operating data for the 2 y before the autopsy was performed are shown in Fig. 2. Missing SWNF data from before April 2007 were due to a later startup for the SWNF train compared to the SWRO train. Unstable SWRO data from February to December 2007 was caused by faulty equipment. Step changes in operating data were responses to deliberate changes in operating conditions. The plant was operated at constant operating conditions over the last 7 months before the autopsy. The specific flux, salt rejections, and differential pressures data for NFP1, NFP2, and SWRO for the last 7 months before the autopsy were steady with no signs of fouling (Fig. 2). Small oscillations followed seasonal changes in temperature and salinity.

Table 2 provides average operating conditions and system performance metrics over the last 7 months of operation. Specific energy consumption (SEC) was calculated from actual flows, pressures, and pump efficiency ratings. Overall, the two-pass SWNF system utilizes about 36% more membrane area to produce about 5% less water, but with slightly higher quality at an energy demand per unit volume of water produced that is only 78% of the SWRO system including the benefits of energy recovery. The overall economics of single-pass SWRO and two-pass SWNF processes will depend on the combined energy reduction and capital cost savings realized by the lower operating pressure in the SWNF system compared to the reduced membrane area enabled by the single pass of SWRO membranes.

3.2. Spiral wound element properties

Digital photographs were taken of membrane leafs after the spiral wound elements were cut open. Fig. 3 shows a picture of each fouled lead membrane element after removing the shell and unrolling the element. The membranes

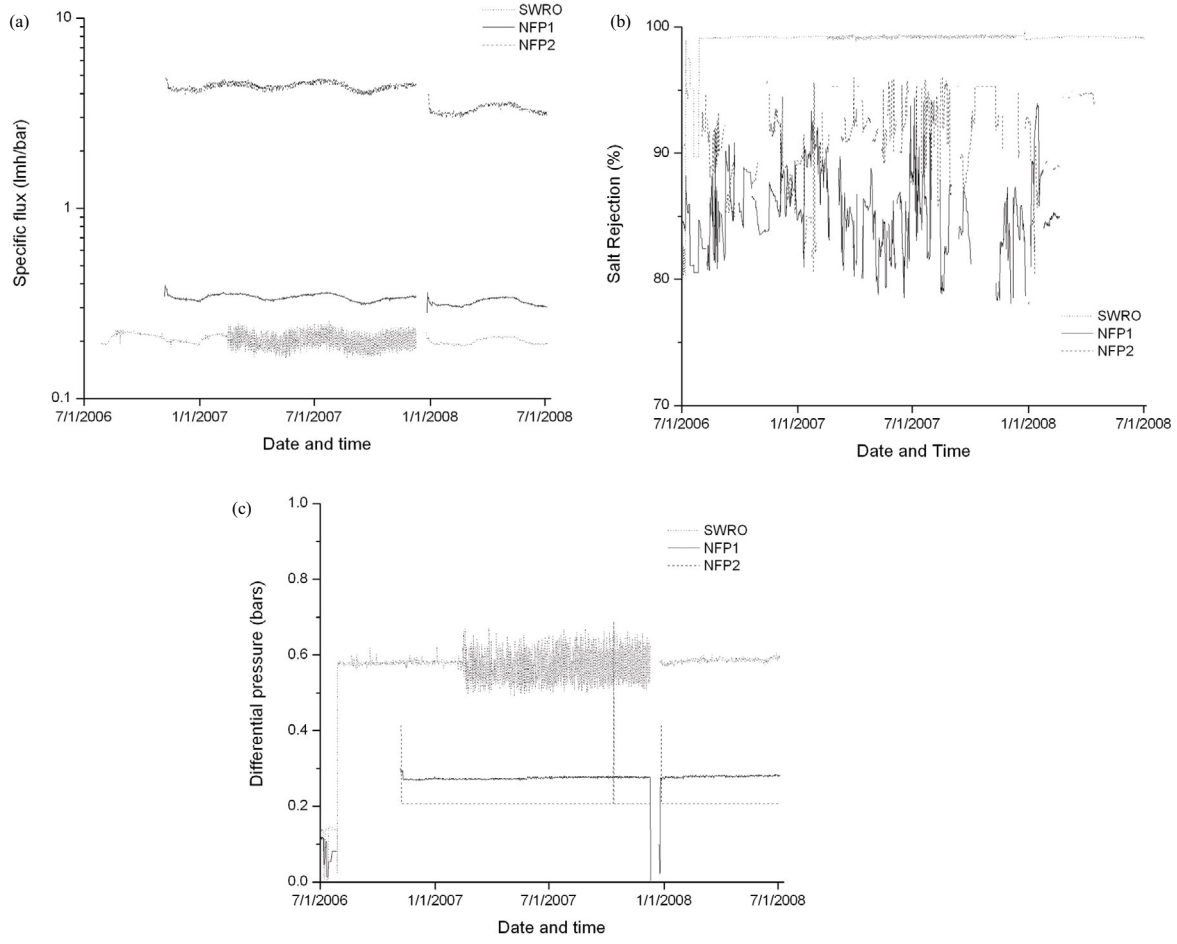

Fig. 2. Operating data from the Long Beach Water Department prototype seawater desalination facility, including (a) specific flux, (b) salt rejection, and (c) differential pressure.

Table 2
Reverse osmosis and nanofiltration membrane properties

Membrane	SWC3+	NF90	NE90
Membrane designation	SWRO	NFP1	NFP2
Location in LBWD prototype	One pass	Pass 1	Pass 2
Manufacturer performance			
Manufacturer	Hydranautics	Dow Water Solutions	Wbongjin Chemical
Maximum operating pressure (bar)	83	41	41
Flux (pm/s)	8.8	8.8	8.3
Nominal rejection	99.7%	85–95%	85–95%
Test conditions	32 g/1 NaCl, 5.5 Mpa	2 g/1 NaCl, 0.48 MPa	2 g/1 NaCl, 0.5 MPa
Feed spacer dimensions			
Spacer thickness, h_c (pm)*	550	650	620
Filament, t/y (pm)*	275	325	310
Configuration	Diamond	Diamond	Diamond
l_a (mm)*	3.0	3.0	3.0
l_b (mm)*	3.0	3.0	3.0
b (°)*	90	90	90
a (°)*	90	90	90
Porosity	0.838 ± 0.009	0.886 ± 0.010	0.839 ± 0.000
Permeate spacer dimensions			
Thickness (pm)	250	230	230
Porosity	0.553 ± 0.007	0.703 ± 0.007	0.693 ± 0.018
Spiral wound leaf dimensions			
Active width (cm)	67.0 ± 0.3	66.6 ± 0.6	86.2 ± 0.4
Active length (cm)	91.1 +/– 0.3	91.6 ± 0.4	90.1 ± 0.7
Leaf area (cm^2)	6,100 ± 37	6,106 ± 40	7,770 ± 70
Number of leaves	29	29	24
Total membrane area			
Measured (m^2)	35.4 ± 0.2	35.4 ± 0.2	45.1 ± 0.4
Reported by manufacturer (tn^2)	37.2	37.2	37.2

*Fig. 4 for illustration.
**"active" = inside glue lines.

(a) (b) (c)

Fig. 3. Fouled membrane images (flow was top to bottom): (a) SWRO, (b) NFP1, and (c) NFP2.

were oriented such that the direction of flow from inlet to outlet was from top to bottom in the pictures. The first element of NFP1 looked similar to the first element of SWRO. Both elements had visible solids build-up especially near the inlet of the elements. The lead element of NFP2 did not appear fouled by visual inspection. As expected, the lead elements looked "more fouled" than the tail elements.

Manufacturer provided specifications for RO and NF membranes used in this project are shown in Table 3 along with the measured spacer and leaf dimensions recorded during the autopsy. Clearly, the NF membranes were not designed for seawater desalination because the manufacturers report performance data from test conditions relevant for brackish water desalination. Fig. 4 illustrates the feed spacer dimensions described in Table 3. The SWRO and NFP1 had similar average active areas per leaf, but different feed spacer thicknesses. The NF membranes both had thicker feed spacers. It was observed that the NF90 offered significantly more membrane area than that reported by the manufacturer, and more membrane than the other membranes based largely on the longer leaf width.

3.3. Fouling layer mass, morphology, and makeup

Fig. 5 shows the volatile (organic), non-volatile (inorganic), and total solids extracted from the membrane surfaces immediately after the elements were opened. The highest concentration of solids was found in SWRO membranes. Similar percentages of solids concentrations found in SWRO were also observed on NFP1 membranes. This suggests that volatile and non-volatile solids fouled both SWRO membrane and SWNF membranes similarly. On NFP2 membranes, total solids buildup was about 60% less than on first pass membranes. In NFP2 membranes, unlike SWRO and NFP1 membranes, non-volatile solids were less than volatile solids. This suggests that most inorganics solids were removed in the first pass of the process, but some organics still reach the second pass NF membrane.

Representative SEM images show the surfaces of unused SWRO, NFP1, and NFP2 in Figs. 6a–c, respectively. The surfaces of SWRO and NFP1 membrane coupons in Figs. 6d and e suggest a large amount of organic deposition. In Fig. 6f, NFP2 has some deposition, but not as much as SWRO and

Table 3
Operating conditions for both trains

	SWRO		SWNF			
	Influent	RO	Influent	Pass 1	Pass 2	Total
Average flow (L/m)	893	337	799	379	265	
Operating Pressure (bar)		49		33.1	15.2	48.3
Recovery (%)		38%		47%	70%	33%
TDS (mg/L)	33,600	260	30,360	4,554	211	
Observed rejection		99.2%		85.0%	95.4%	99.3%
Number of vessel in parallel		8		8	4	
Stage 1 Number of elements per vessel		5		5	5	
Number of element		40		40	20	
Number of vessel in parallel		8		8	6	
Stage 2 Number of elements per vessel		2		2	0	
Number of element		16		16	0	
Average flux (pm/s)		2.8		2.8	7.5	
SEC (kWh/m^3)		4.8		2.6	0.8	3.4
SEC with ER (kWh/m^3)		3.2		1.9	0.7	2.5

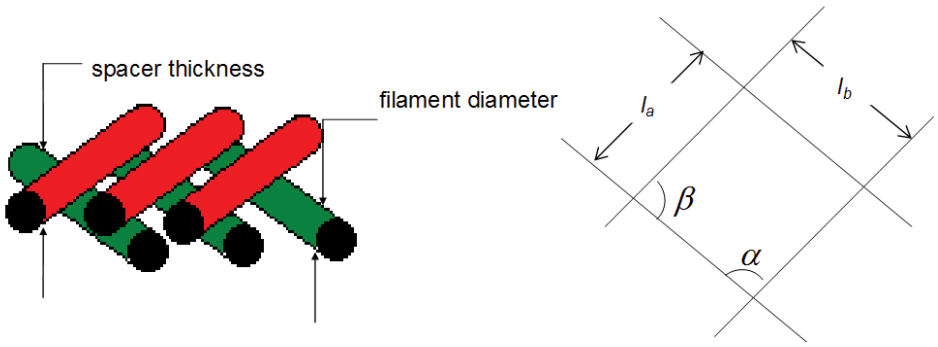

Fig. 4. Illustration of feed spacer dimensions described in Table 2.

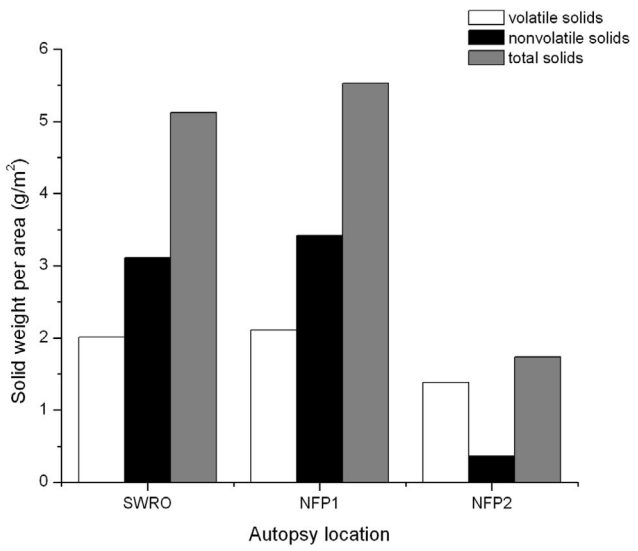

Fig. 5. Weight of solids per unit area on lead membrane elements.

NFP1. Large NaCl crystals were present on the surfaces of all the membrane samples. It was suspected that these crystals appeared when membrane samples were dried prior to sputter coating for the SEM because the membranes were not rinsed before drying. Commercially cleaned membrane surfaces in Figs. 6g and h still have some solid buildup on the membrane surfaces. At lower magnifications, feed spacer patterns were visible on the membrane surfaces. Fouling was most severe where feed spacers left an impression on the membranes suggesting the spacers promote localized solids accumulation.

Elemental analysis by EDX (Fig. 7a) indicated sodium, chloride, iron, and chromium were detected on surfaces of NFP1 membranes, while sodium, chloride, iron, and bromide were detected on surfaces of SWRO membranes. Carbon and oxygen derive from the polyamide and polysulfone polymers as well as organic foulants and oxides. Sulfur is predominantly from the polysulfone support layer. The ratio of C:O:S changes between the unused, fouled, and cleaned membranes. Both unused SWRO and NFP1 membranes have the highest C:O ratio. Fouled SWRO and NFP1

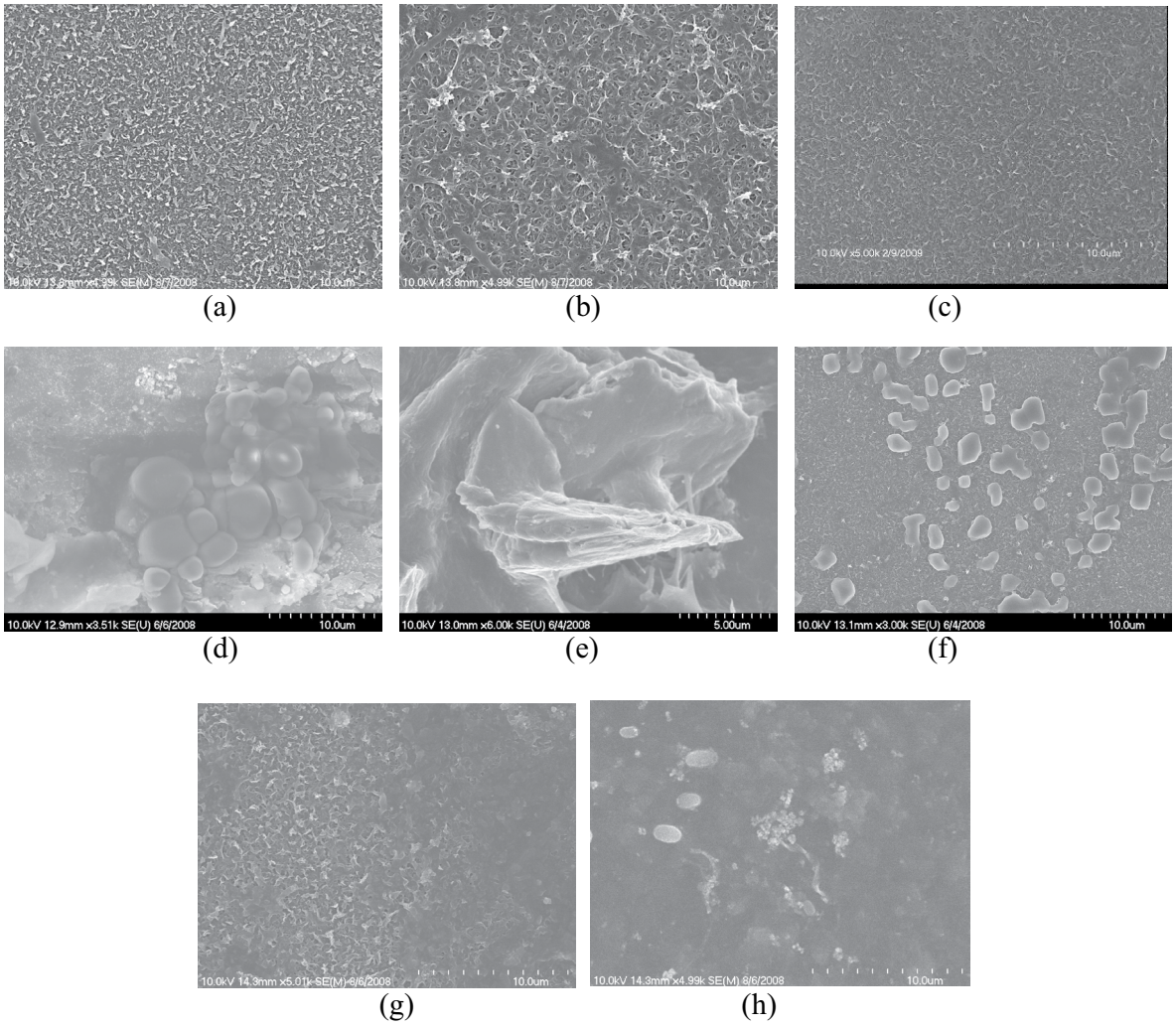

Fig. 6. Representative SEM images of unused (a) SWRO, (b) NFP1, and (c) NFP2 membrane samples, fouled (d) SWRO, (e) NFP1, and (f) NFP2 lead elements, and chemically cleaned (g) SWRO and (h) NFP1 first-pass lead elements.

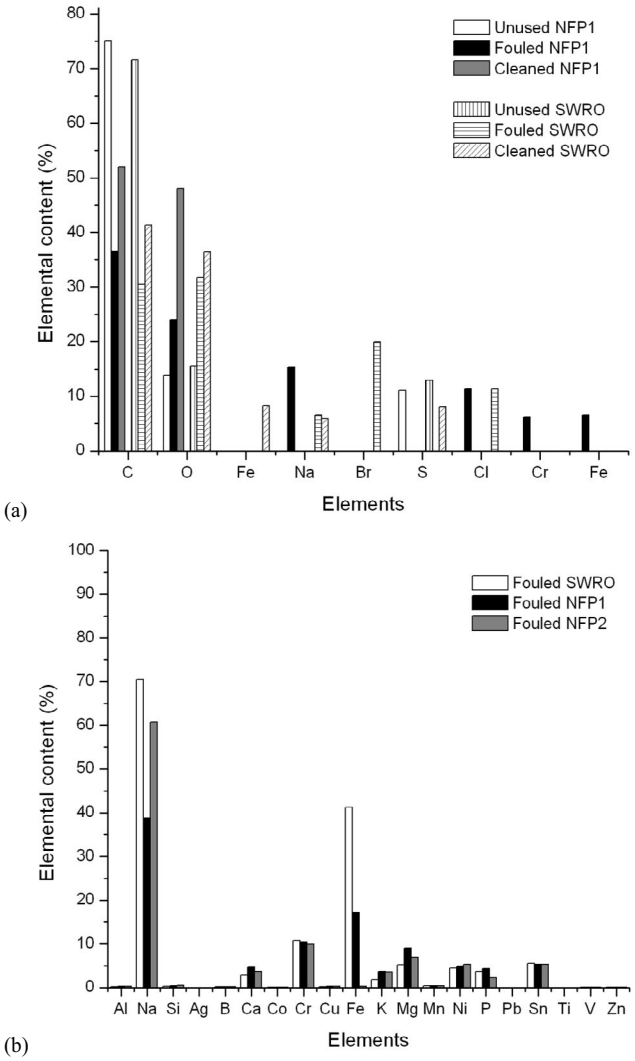

Fig. 7. Elemental analyses of unused, fouled, and cleaned membranes by (a) EDX and (b) ICP.

have reduced C:O ratio. This may be caused by buildup of hydroxyl rich organics, plus mineral oxides, hydroxides, carbonates, sulfates, and silicates. The C:O ratio for cleaned membranes was about the same as the fouled membrane, which suggests that either the fouling material was not removed by chemical cleaning or the membrane chemistry changed. Similar to EDX results, elemental analyses by ICP (Fig. 7b) suggest that sodium and iron accumulated on all of the membranes. Calcium, potassium, and magnesium found in the EDX analyses are major ions in seawater. Nickel, phosphorous, and tin found may be contributed from the trace elements in seawater.

Sodium and chloride are most likely precipitated during sample preparation as discussed above. Iron and chromium occur naturally in Long Beach seawater, but could also be corrosion products from stainless steel components of the plant. In addition, iron precipitation can occur when chlorination of the MF feed water fails. Typically, with proper chlorination, naturally occurring dissolved iron in seawater oxidizes, precipitates as iron hydroxide particles, and is rejected by MF pretreatment membranes [15]. However, occasionally the chlorine injection system malfunctioned, and the feed water was not chlorinated, and hence, dissolved iron could have passed through MF pretreatment and accumulated on the membrane surface.

Results from FTIR analyses of unused and fouled membranes are presented in Fig. 8. Light (red) lines represent unused membranes and the dark (blue) lines are fouled membranes. The peak at 1,245 cm^{-1} is the C–O–C bending vibration from the polysulfone support layer of the composite RO membrane [16]. The absorbance at 1,245 cm^{-1} is lower on the fouled membranes because the foulant layer covering the membrane limits the penetration depth of the infrared beam into the polysulfone support. Therefore, the extent of this characteristic peak reduction gives some indication of the fouling layer thickness.

Distinctly enhanced absorbance was observed at 1,650 cm^{-1} (amide I), 1,550 cm^{-1} (amide II), which are indicative of proteins [17,18]. The C–O stretching band associated with carbohydrate or polysaccharides is near 1,040 cm^{-1} [18]. The band in between 600 and 800 cm^{-1} could be due to the aromatic backbone of polyamide [19]. An enhancement of absorbance around 3,300–3,400 cm^{-1} is also significant, which might indicate hydroxyl groups of polysaccharides [20]. Overall we deduce from the three FTIR spectra in Fig. 8 possible accumulation polysaccharide and proteinaceous materials on the membranes. The NFP2 spectra suggest a much thinner fouling layer, which is consistent with the solids analyses and SEM images.

Commercially cleaned NFP1 and SWRO membrane FTIR results are plotted in Fig. 9 in the form of a difference spectrum. Note the *Y*-axis values used here are relative. Dark (blue) lines represent the difference between spectra obtained from fouled and unused membranes (fouled-unused), while light (green) lines indicate the difference in spectra from cleaned and unused membranes (cleaned-unused). Fouled and cleaned difference spectra for NFP1 membranes were almost identical, which suggests the cleaning was relatively ineffective. However, the fouled and cleaned SWRO membrane difference spectra were very different; the cleaned-unused spectra was almost flat, which indicates SWRO membranes were very effectively cleaned.

3.4. Biological analyses

Representative fluorescence microscopy images of fouled (Fig. 10) and cleaned (Fig. 11) membranes stained by fluorescent molecular probes show both live and dead cells accumulated on all membranes. White spots on the microscopic images are bacteria cells. Direct cell counts from these images are provided in Table 4. Many fewer cells were found on the NF membranes, but we are not certain the difference is statistically significant. The slightly higher cell count on the cleaned NFP1 membrane definitely falls within the level of accuracy of the direct cell counting method, so this is probably not a real trend. Live, viable bacteria were identified on all membrane surfaces – both before and after cleaning – suggesting that bacteria colonized the membrane surfaces of all three membranes (only lead elements were tested) and that cleaning did not remove the adhered bacteria cells. However, without identifying

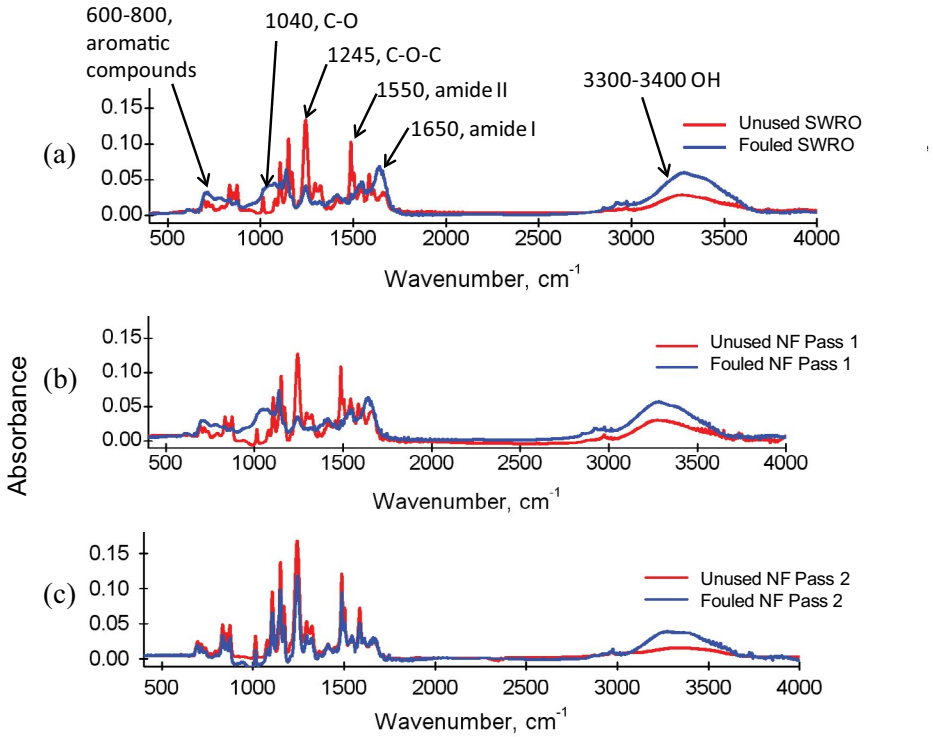

Fig. 8. FTIR analyses of unused and fouled (a) SWRO, (b) NFP1, and (c) NFP2 membranes.

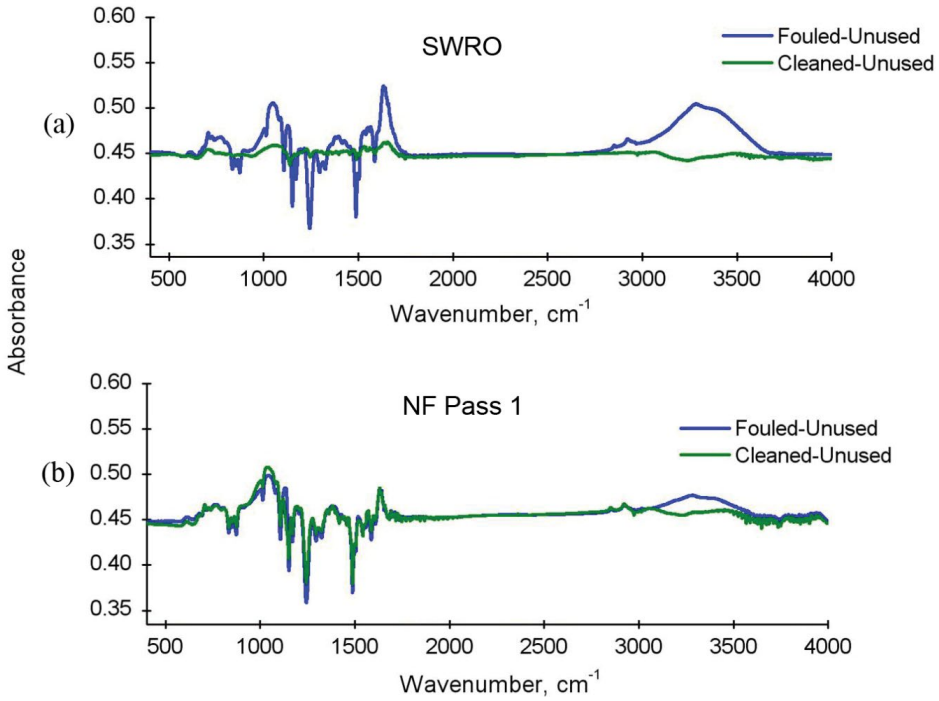

Fig. 9. FTIR difference spectra from unused, fouled, and cleaned (a) SWRO and (b) NFP1 membranes.

the nature of the bacteria one cannot rule out laboratory contamination as the source of all bacteria cells.

Since both live and dead bacteria were found on all membrane surfaces, bacterial cultures were prepared to identify the origin and type of bacteria. Morphological characteristics of the four bacteria isolates are described in Table 5 and cell culture plates are shown in Fig. 12. Phylogenetic analyses of cultured cells (Fig. 13) suggest all four bacteria

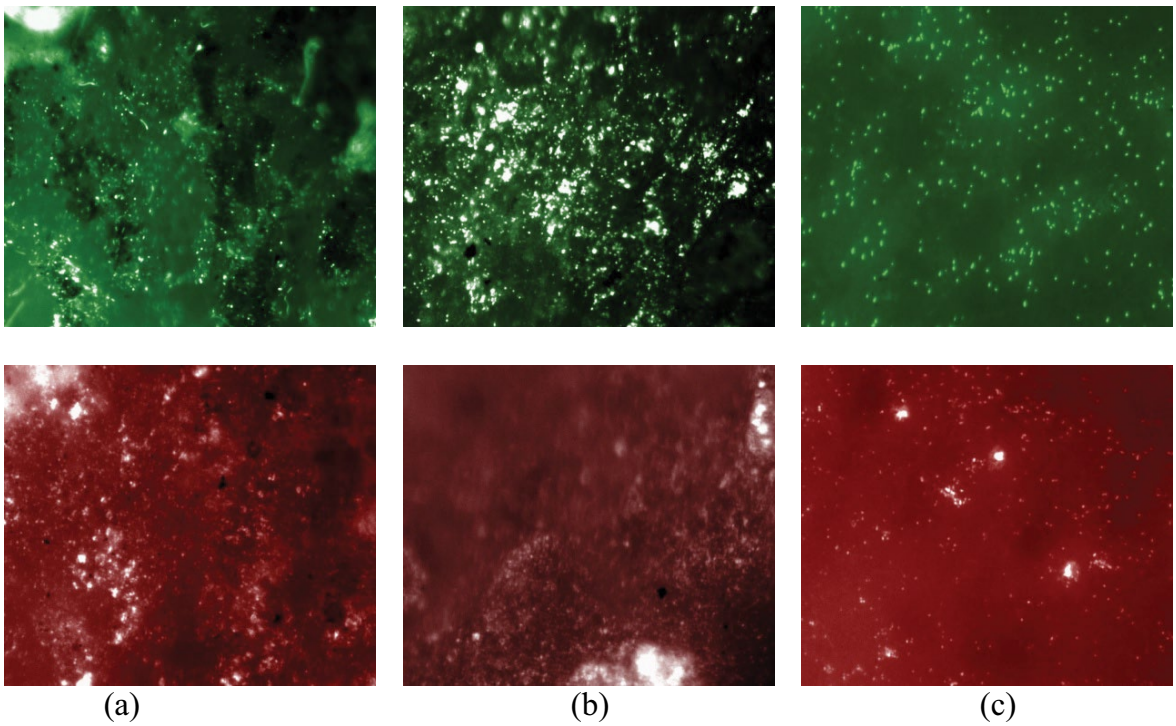

Fig. 10. Live (top) and dead (bottom) bacteria cells on fouled (a) SWRO, (b) NFP1, and (c) NFP2 membranes.

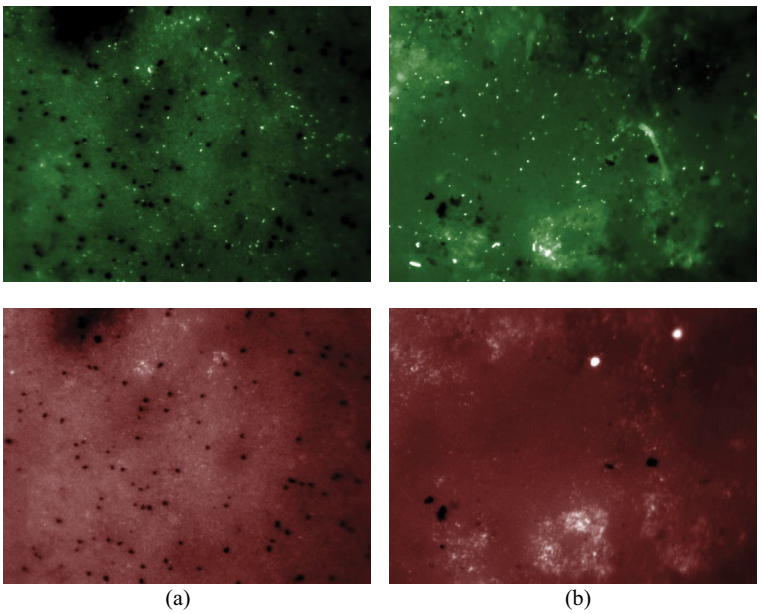

Fig. 11. Live (top) and dead (bottom) bacteria cells on cleaned (a) SWRO and (b) NFP1 membranes.

were related to known marine bacteria. Samples S1 and S2 (Table 5) were similar and identified as *Muricauda* spp. The genus *Muricauda* is a member of the family *Flavobacteriaceae* within the *Cytophaga–Flavobacterium–Bacteroides* (CFB) complex [21]. The strain that matched closest to our isolates, *Muricauda aquimarina*, was previously isolated from the sea surface microlayer of the northwestern Mediterranean Sea [22]. Bacteria similar to *Muricauda* spp. have been previously identified in mature marine biofilm covering a rock-bed of the East Sea in Korea [23]. However, the colony pigment of this previous isolate was orange on marine agar, which is different from the yellow-colored colony displayed by S1 and S2. Samples S3a and S3b belong to marine *Bacillus* spp., most closely related to *Bacillus aquimaris* previously isolated from a tidal flat of the Yellow Sea in Korea [24]. *Bacillus* spp. are known to form biofilms in food industries [25] and

Table 4
Live and dead staining results for fouled membranes and cleaned membranes

Membrane	Fouled membranes		Commercially cleaned membranes	
	Live (#/mm^2)	Dead (#/mm^2)	Live (#/mm^2)	Dead (#/mm^2)
First element of SWRO (SWC3+)	637	346	71	25
First element of NF Pass 1 (NF90)	31	433	88	141
First element of NF Pass 2 (NE90)	48	52	NA	NA

"NA" = not analyzed; "#" = number of cells.

Table 5
Cultured bacteria source and morphology

Sample designation	Sample location	Colony morphology
S1	SWC3+ last element second stage	Small yellow colony, translucent with a smooth edge
S2	NF90 first element from the first stage	Small yellow colony, translucent with a smooth edge
S3a	SWC3+ first element from the first stage after commercial cleaning	Medium pink colony, opaque center with the clear ring, and smooth edge
S3b	SWC3+ first element from the first stage after commercial cleaning	Large opaque colony with dense center and smooth edge

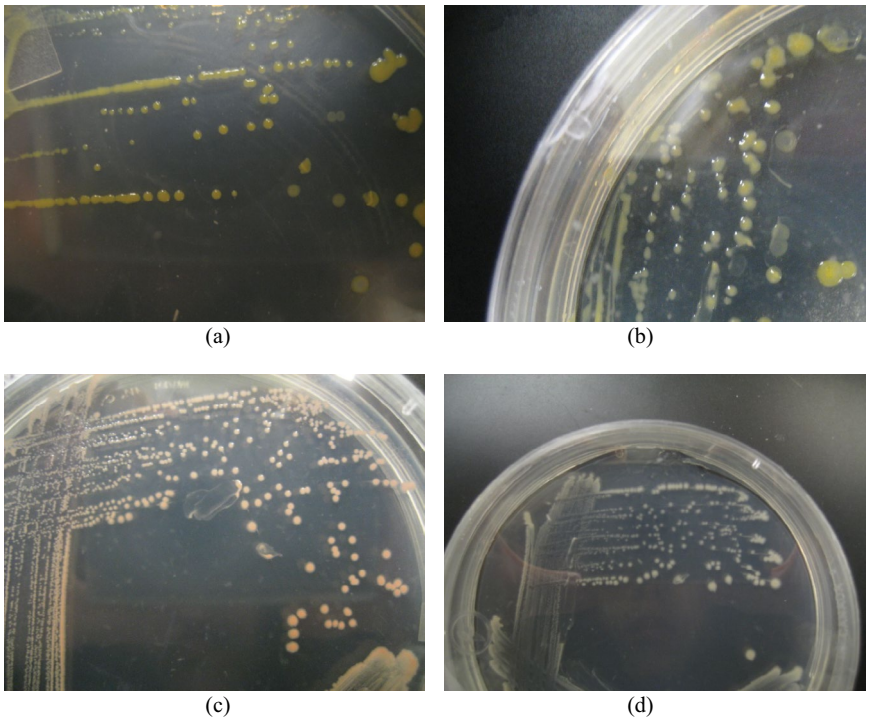

Fig. 12. Bacteria cultures for (a) SWRO (S1), (b) NFP1 (S2), and (c and d) commercially cleaned SWRO membranes (S3a and b).

clinical microbiology [26] as well as in previous RO membrane autopsies [27]. Some marine *Bacillus* were previously identified from marine biofilms [28].

Biofilm isolates matched closely to known marine bacteria from previous studies, suggesting that they are commonly cultivable bacteria in seawater. However, cultured microbes may not represent the total bacterial community since over 99% of marine bacteria are not cultivable on artificial medium. It is unclear how viable, culturable bacteria passed through microfiltration and disinfection pretreatments to colonize the membranes, but it appears that they did. Additional studies on their sizes and resistance to disinfection may provide further understanding of their origin and persistence. Phylogenetic analysis showed that

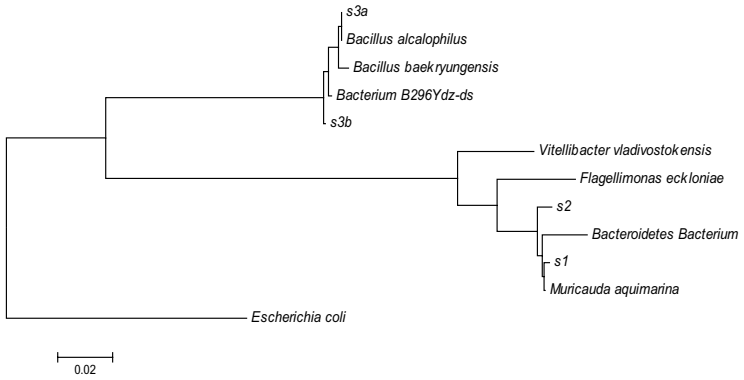

Fig. 13. Phylogenetic relationship of bacterial isolates relative to known bacteria in the GenBank database.

Table 6
Results from laboratory and commercial membrane cleaning

Description SWRO	Flux (pm/s)	*A* (pm/s bar)	Rejection (%)	*B* (pm/s)
Unused membrane	17.8	0.431	99.18%	0.147
Fouled membrane	17.3	0.417	99.47%	0.092
Laboratory (UCLA) cleaned membrane after NaOH	19.8	0.479	N/A	N/A
Laboratory (UCLA) cleaned membrane after citric acid	19.6	0.475	99.25%	0.148
Commercially cleaned membrane	24.3	0.587	99.96%	0.010
NF Pass 1				
Unused membrane	46.6	1.126	93.52%	3.227
Fouled membrane	30.7	0.741	96.52%	1.106
Laboratory (UCLA) cleaned membrane after NaOH	54.8	1.324	N/A	N/A
Laboratory (UCLA) cleaned membrane after citric acid	55.8	1.349	95.82%	2.434
Commercially cleaned membrane	52.2	1.261	99.79%	0.109
NF Pass 2				
Unused membrane	66.7	1.611	93.28%	4.802
Fouled membrane	55.9	1.351	92.84%	4.309
Laboratory (UCLA) cleaned membrane after NaOH	64.5	1.559	N/A	N/A
Laboratory (UCLA) cleaned membrane after citric acid	68.3	1.651	92.88%	5.231
Commercially cleaned membrane		Not autopsied		

Note the following test conditions:
Applied pressure = 41 bars.
Temperature = 25°C.
Feed NaCl concentration = 32,000 mg/L.
Feed pH = 6.0 ± 0.2.

all isolates represent genus that have demonstrated biofilm formation potential, suggesting our isolates are potential contributors to membrane fouling.

3.5. Membrane cleaning results

Table 6 presents fluxes, rejections, and permeability coefficients for unused, fouled, and cleaned membranes. Fouled membranes were cleaned separately in the laboratory UCLA and at Siemens. In the laboratory, the NaOH solution was more efficient at recovering the initial membrane permeability than the citric acid solution. It is well-known that caustic solublizes organic and biological matter, whereas acids are effective for digesting minerals and metals. These cleaning results further indicate that organic and biological matter were the predominant cause of fouling. The chemical cleaning procedure employed in the laboratory at UCLA did not fully recover the clean membrane salt rejection for SWRO and NFP1 membranes.

The commercially cleaned NFP1 membranes were returned with a report that averaged a decrease in salt rejection after the cleaning from 97.4% (fouled) to 96.4% (cleaned). The testing result at UCLA for commercially cleaned NFP1 membranes reported an increase from 96.5% (fouled) to 99.8% (cleaned). Both the commercial cleaning report and the UCLA flat sheet performance test revealed that the

commercial cleaning was more effective than the UCLA cleaning method at recovering the flux and rejection. The temperature for the commercial cleaning was 43°C–49°C, whereas at UCLA, the cleaning solution temperatures were maintained at 25°C. The rate of chemical reaction between cleaning agents and foulants, the mass transfer of foulants from the fouling layer to the bulk solution, and the solubility of foulant materials during cleaning all increase with temperature [29]. Further, the commercial cleaning time was at 2 h. At UCLA the cleaning time was 30 min. Finally, the commercial cleaning protocol may involve more complex chemical mixtures including enzymes, surfactants, and chaotropic agents.

4. Conclusions

Autopsy analyses of unused, fouled, and cleaned NF and RO membranes used in a prototype seawater desalination system suggest the following.

- Plant operating data did not suggest outward signs of membrane fouling, while autopsy analyses identified organic, inorganic, and biological matter on all membranes analyzed. This observation was theoretically predicted by Chen et al. [6]. Additional research is needed to improve early detection of fouling and incorporating such feedback into plant optimization and control systems.
- At least for this water source and these membranes over the operating period investigated, viable, culturable biofim forming marine bacteria were isolated from all membranes. No outward symptoms of membrane fouling were observed at the plant. Better methods of detecting initial bacterial colonization are needed.
- None of the chemical cleaning regimens employed were able to remove the bulk of foulant mass from seawater NF membranes. Viable, culturable biofilm forming marine bacteria remained on both NF and RO membranes after cleaning. Chemical cleaning protocols must be improved to (a) target the removal of attached bacterial cells from both RO and NF membranes and (b) achieve better removal of organic matter from seawater NF membranes.

It may be unwise to draw broad, generalized conclusions from this study about the mechanisms of membrane fouling or the effectiveness of membrane cleaning at all seawater desalination plants – particularly because there were no plant level indications of membrane fouling in this study. Since the total system flux is not a reliable indicator of seawater NF/RO membrane fouling, future research on seawater NF/RO membrane fouling may consider better process monitoring devices, fouling detectors, to enable early warning detection of biofouling and to help optimize and improve chemical cleaning methods.

Acknowledgments

Financial support for this work was provided by Long Beach Water Department. In addition, we are grateful to: (a) Dow Water Solutions, Woongjin Chemical, and Hydranautics for supplying unused membrane samples, (b) Greg Guillen, Dr. Vinh Nguyen, Breanne Born, Gil Hurwitz, and Dr. Mary Laura Lind from the Department of Civil and Environmental Engineering at UCLA for their help in the autopsy process, (c) Jose Sanchez, Carlos Ibarra, and John Myers from the UCLA School of Engineering and Applied Science (SEAS) machine shop for their help to autopsy the membrane, and (d) Tai Tseng and Cynthia Andrews-Tate from Long Beach Water Department for providing used membrane elements, water quality analyses, and operating data from the prototype desalination system.

References

[1] P.H. Gleick, The World's Water, 2006–2007: The Biennial Report on Freshwater Resources, Island Press, Washington, DC, 2006.
[2] G. Guillen, E.M.V. Hoek, Modeling the impacts of feed spacer geometry on reverse osmosis and nanofiltration processes, Chem. Eng. J., 149 (2009) 221–231.
[3] M. Busch, W.E. Mickols, Reducing energy consumption in seawater desalination, Desalinatio, 165 (2004) 299–312.
[4] C. Harris, Energy recovery for membrane desalination, Desalination, 125 (1999) 173–180.
[5] C.J. Harrison, Y.A. Le Gouellec, R.C. Cheng, A.E. Childress, Bench-scale testing of nanofiltration for seawater desalination, J. Environ. Eng., 133 (2007) 1004–1014.
[6] K.L. Chen, L.F. Song, S.L. Ong, W.J. Ng, The development of membrane fouling in full-scale RO processes, J. Membr. Sci., 232 (2004) 63–72.
[7] E.M.V. Hoek, J. Allred, T. Knoell, B.-H. Jeong, Modeling the effects of fouling on full-scale reverse osmosis processes, J. Membr. Sci., 314 (2008) 33–49.
[8] T. Someya, K. Inubushi, H. Yamamoto, K. Kato, Recent advances in the study on viable but nonculturable (VBNC) microorganisms in aquatic and soil environments, Soil Microorg., 53 (1999) 45–51.
[9] M. Troussellier, J.L. Bonnefont, C. Courties, A. Derrien, E. Dupray, M. Gauthier, M. Gourmelon, F. Joux, P. Lebaron, Y. Martin, M. Pommepuy, Responses of enteric bacteria to environmental stresses in seawater, Oceanol. Acta, 21 (1998) 965–981.
[10] D.X. Vuong, Two Stage Nanofiltration Seawater Desalination System, US Patent Office, City of Long Beach (Long Beach, CA, US), United States, 2006.
[11] R.A. Horne, Marine Chemistry: The Structure of Water and the Chemistry of the Hydrosphere, Wiley-Interscience, New York, NY, 1969.
[12] L.S. Clesceri, A.E. Greenberg, A.D. Eaton, M.A.H. Franson, American Public Health Association, American Water Works Association, Water Environment Federation, Standard Methods for the Examination of Water and Wastewater, 20th ed., American Public Health Association, Washington, DC, 1998.
[13] E. Stackebrandt, M. Goodfellow, Nucleic Scid Techniques in Bacterial Systematics, Wiley, Chichester; New York, NY, 1991.
[14] X. Jin, A. Jawor, S. Kim, E.M.V. Hoek, Effects of feed water temperature on separation performance and organic fouling of brackish water RO membranes, Desalination, 239 (2009) 346–359.
[15] K.-H. Choo, H. Lee, S.-J. Choi, Iron and manganese removal and membrane fouling during UF in conjunction with prechlorination for drinking water treatment, J. Membr. Sci., 267 (2005) 18–26.
[16] A.P. Rao, S.V. Joshi, J.J. Trivedi, C.V. Devmurari, V.J. Shah, Structure-performance correlation of polyamide thin film composite membranes: effect of coating conditions on film formation, J. Membr. Sci., 211 (2003) 13–24.
[17] H.H. Mantsch, D. Chapman, Infrared Spectroscopy of Biomolecules, Wiley-Liss, New York, NY, 1996.
[18] C. Jarusutthirak, G. Amy, Role of soluble microbial products (SMP) in membrane fouling and flux decline, Environ. Sci. Technol., 40 (2006) 969–974.

[19] T. Tran, B. Bolto, S. Gray, M. Hoang, E. Ostarcevic, An autopsy study of a fouled reverse osmosis membrane element used in a brackish water treatment plant, Water Res., 41 (2007) 3915–3923.
[20] S. Mondal, S.R. Wickramasinghe, Produced water treatment by nanofiltration and reverse osmosis membranes, J. Membr. Sci., 322 (2008) 162–170.
[21] A. Bruns, M. Rohde, L. Berthe-Corti, *Muricauda ruestringensis* gen. nov., sp nov., a facultatively anaerobic, appendaged bacterium from German North Sea intertidal sediment, Int. J. Syst. Evol. Microbiol., 51 (2001) 1997–2006.
[22] H. Agogue, F. Joux, I. Obernosterer, P. Lebaron, Resistance of marine bacterioneuston to solar radiation, Appl. Environ. Microbiol., 71 (2005) 5282–5289.
[23] K.K. Kwon, Y.K. Lee, H.K. Lee, *Costertonia aggregata* gen. nov., sp nov., a mesophilic marine bacterium of the family *Flavobacteriaceae*, isolated from a mature biofilm, Int. J. Syst. Evol. Microbiol., 56 (2006) 1349–1353.
[24] J.H. Yoon, I.G. Kim, K.H. Kang, T.K. Oh, Y.H. Park, *Bacillus marisflavi* sp nov and *Bacillus aquimaris* sp nov., isolated from sea water of a tidal flat of the Yellow Sea in Korea, Int. J. Syst. Evol. Microbiol., 53 (2003) 1297–1303.
[25] Y.H. Hsueh, E.B. Somers, D. Lereclus, A.C.L. Wong, Biofilm formation by Bacillus cereus is influenced by PlcR, a pleiotropic regulator, Appl. Environ. Microbiol., 72 (2006) 5089–5092.
[26] K.P. Lemon, A.M. Earl, H.C. Vlamakis, C. Aguilar, R. Kolter, Biofilm development with an emphasis on *Bacillus subtilis*, Corr. Top. Microbiol. Immunol., 322 (2008) 1–16.
[27] A. Subramani, E.M.V. Hoek, Direct observation of initial microbial deposition onto reverse osmosis and nanofiltration membranes, J. Membr. Sci., 319 (2008) 111–125.
[28] Y.K. Lee, K.K. Kwon, K.H. Cho, J.H. Park, H.K. Lee, Isolation and identification of bacteria from marine biofilms, Key Eng. Mater., 277–279 (2005) 612–617.
[29] W.S. Ang, S. Lee, M. Elimelech, Chemical and physical aspects of cleaning of organic-fouled reverse osmosis membranes, J. Membr. Sci., 272 (2006) 198–210.